

Multiphysics Enabled Numerical Modeling of a Plasma Based Electrically Small VHF-UHF Antenna

Samsud Moon
mmoon4@rockets.utoledo.edu

Abstract—A three-dimensional model of a novel plasma based electrically small antenna is developed for investigating the gas properties and antenna parameters under a low pressure, low plasma temperature environment. The antenna exhibits dipole antenna-like behavior with wide-band impedance matching from 213 – 700 MHz. Plasma is sustained by 0.9 W of RF input power at 100 MHz and the gas pressure is strategically controlled at 500 mili-Torr. The simulated S_{11} is verified against the available experimental data and further antenna parameters are extracted. The proposed ESA shows dipole-like radiation pattern with a radiation efficiency of 16% at 700 MHz. The performance metric for ESAs, the Chu-limit, is exceeded by this antenna with the $Bandwidth \times Efficiency$ reaching 0.168 with a ka of 0.5571. The findings from this letter demonstrate the practicability of using COMSOL Multiphysics as a tool for predicting plasma behavior and antenna performance while the boundary conditions for all the coupled physics are respected.

Index Terms—Numerical modeling, antenna, plasma, electrically small, VHF,UHF

I. INTRODUCTION

The demand for antennas that are electrically small (ESA) is ever increasing due to their capability of being used in various applications where conventional antennas are too large for the frequency. ESAs are small, making them useful for devices of compact size. ESAs suffer from several setbacks like low efficiency and narrow bandwidth, mostly resulting from inefficient design and extreme difficulty in wide-band impedance matching.

Several impedance matching schemes have been proposed previously by [1], [4] where negative impedance converters are used for wide-band matching. A novel approach to tackle the narrow bandwidth for small antennas was proposed in [2], [9] where the frequency dependent complex impedance is matched by capacitively-coupled plasma for a wide range of bandwidth. The capacitive structure with above threshold electron density allows the bulk plasma to act as a negative capacitance [6], which alleviates the effect of negative complex impedance for such an ESA.

Due to the instabilities of extreme low pressure plasma, antenna measurements inside an anechoic chamber faces significant hurdles. At milli-Torr level pressures, a plasma standalone device loses most of its gas molecules due to de-gassing of the inert gas to the dielectric wall overtime. Maintaining the pressure inside the plasma cell becomes challenging without a pressure controlled gas chamber. These

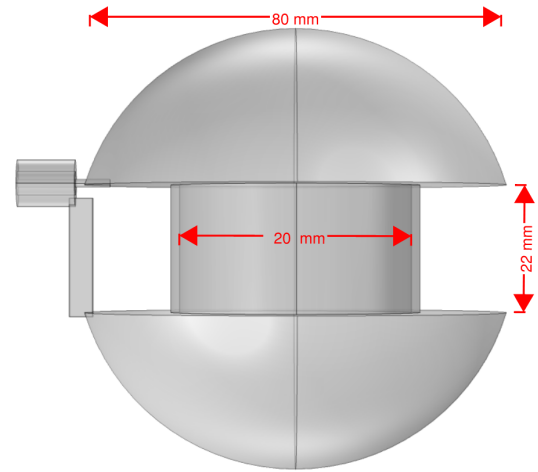


Fig. 1. 3D model of the capped dipole ESA.

gas chambers are often made of metal which interfere with the antenna performance, hence distorting the measurement.

This work proposes a simplified approach to measuring plasma and antenna parameters under anechoic chamber conditions. A 3D model for a reference antenna from [5] is simulated under low pressure, low plasma temperature condition with the help of commercially available software, COMSOL Multiphysics [3]. The simulated results are verified against the antenna reflection measurement and typical antenna parameters are extracted from the validated numerical model.

II. MODEL DESCRIPTION

A. Geometry

The antenna model follows identical parameters of that of [5]. A plasma cell of radius of 20 mm and a height of 22 mm is sandwiched by two semi-spherical copper electrodes, encompassing an antenna of 80 mm diameter, as shown in Figure-1. An absorbing layer with 300 mm radius and 30 mm thickness is defined at the antenna far-field region. The plasma is housed by a 1.5 mm thick pyrex tube radially. The RF power is provided by the coaxial port in the left.

B. Physics

Two different physics modules, 'Electromagnetic Waves, Frequency Domain (emw)' and 'Plasma (plas)' were coupled

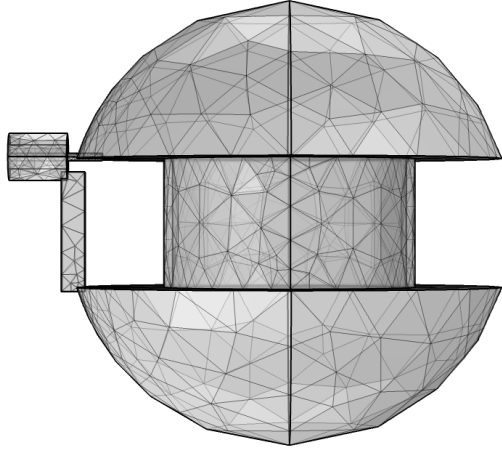


Fig. 2. Custom user-controlled mesh of the ESA structure.

together in this modeling. The emw module is used for the ignition of the gas, and to measure antenna parameters like reflection, impedance and radiation pattern. The plasma module calculates the plasma electron number density, electron temperature, density profile and many other plasma parameters. The RF power through the coaxial port acts as the electron heat source.

C. Mesh

Like any other numerical modeling technique, COMSOL has some trade-off between the computation time and accuracy. However, the flexibility of choosing different mesh for different domains aids in reducing the computational burden without sacrificing significant accuracy. For this model, the physics dependent custom mesh consists of 21417 domain elements, 3510 boundary elements, and 632 edge elements. Figure-2 depicts the meshing scheme for an accurate and quick solution for a critical antenna structure like a plasma antenna. It can be noted that the plasma domain mesh is much finer than that of the electromagnetic domain.

D. Study

The model consists of two studies. First, the whole ESA is simulated without the presence of plasma. The plasma domain is assumed to be vacuum with similar relative permittivity. This study provides the electromagnetic domain simulation of a conventional dipole antenna. The next study is carried out in two steps. First, the plasma is ignited by providing a single frequency RF power and continues until a steady state background gas solution is reached. The last time step provides the plasma parameters in steady state. The solution is stored. The second step uses the stored solution data, and calculates the electromagnetic properties of the antenna keeping the steady plasma as a background gas. This step provides the plasma antenna parameters with plasma in on state.

In the next section, the simulation results are provided and compared to the experimental results from [5].

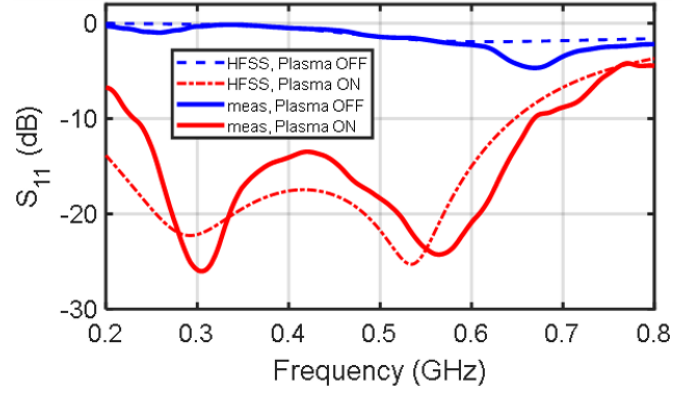


Fig. 3. Measured and HFSS simulated reflection coefficients for plasma ESA [9].

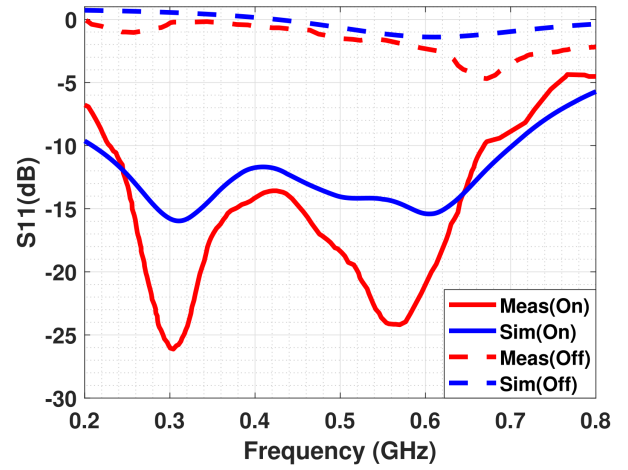


Fig. 4. Comparison of measured and COMSOL simulated results.

III. RESULT ANALYSIS

A. Antenna Reflection

As produced in figure-3 from [9], the antenna has a reflection less than -10 dB from 230 MHz till 667 MHz. The results from the COMSOL simulation and experimental measurement are compared in figure-4. The COMSOL simulated result and the measured result are under good agreement for the frequency range of 0.2-0.8 GHz. This comparison serves as a validation of the accuracy of the proposed 3D model and simulation setup. The plasma was ignited and sustained with 0.9 W of RF power at 100 MHz of excitation signal. The background gas, Ar, was kept at a pressure of 0.5 Torr. Under these parameters, the plasma electron number density profile provided a Maxwellian distribution as depicted by figure-5 with a maximum electron number density of $1.77 \times 10^{17} m^{-3}$ at the center of the discharge. This electron density assisted in matching the real and imaginary part of the plasma impedance, which can be modeled with the following terms [8],

$$\epsilon_{rp} = 1 - \frac{e^2 n_e}{\epsilon_0 m (\omega^2 + \nu_m^2)}, \quad (1)$$

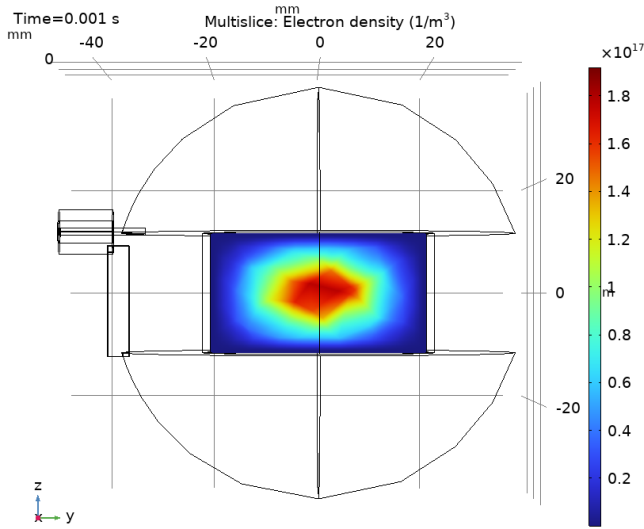


Fig. 5. 3D electron number density profile over the discharge gap.

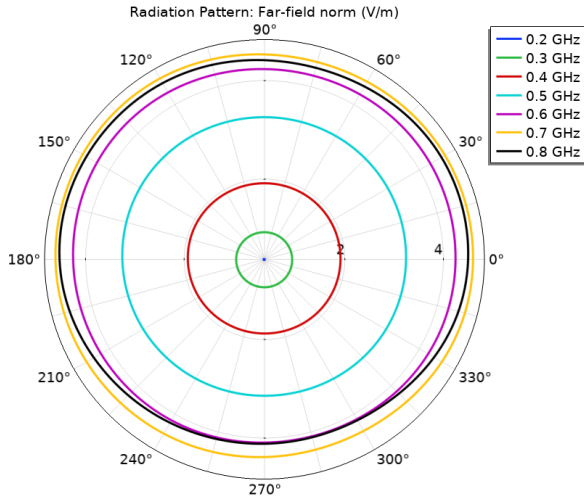


Fig. 6. Far field radiation pattern at intermediate frequencies.

$$\sigma_p = \frac{e^2 n_e v_m}{m(\omega^2 + v_m^2)}, \quad (2)$$

where ϵ_{rp} is relative permittivity, σ_p is electrical conductivity, and n_e is the electron number density. v_m is the electron-neutral collision frequency and ω is the EM frequency. The simulated antenna has less than -10 dB reflection over the frequency range of 213 MHz to 700 MHz, with a fractional bandwidth of 106.67%.

B. Radiation Pattern

The simulated radiation pattern of the ESA at intermediate frequencies are plotted in figure-6 and 7. The realized far field gain is maximum at 0.7 GHz and the 3D gain pattern is shown for this frequency.

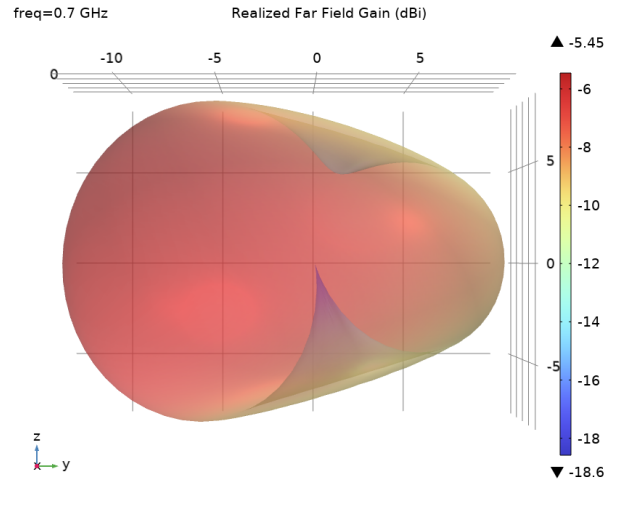


Fig. 7. 3D Far field gain at 0.7 GHz.

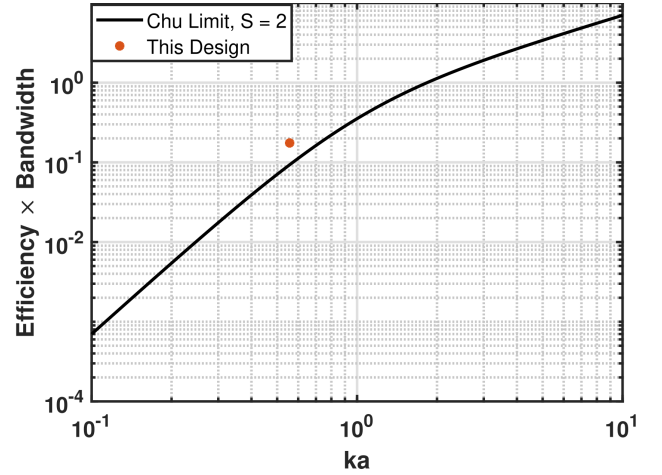


Fig. 8. Performance measure for the simulated electrically small antenna.

The antenna efficiency can be derived from the following formula,

$$\frac{\text{Antenna Gain}}{\text{Directivity}} = \text{Antenna Efficiency}$$

The realized far field gain extracted from Fig. 7, $Gain_{max} = -5.45$ dBi, and directivity at 0.7 GHz, $D_{0.7} = 2.5735$ dB yields a radiation efficiency of 0.16 at the specific frequency. Comparing this antenna to conventional electrically small antennas, this design was found to substantially exceed the Chu-limit [7] at a ka of 0.5571, as shown in Fig. 8, where a is the antenna radius and k is wave number. Although this is a fundamental limit, the antenna is able to exceed it theoretically because of its unconventional matching technique and efficient use of the total antenna volume.

IV. CONCLUSION

Antenna measurement is a delicate process due to the omnipresence of electromagnetic interference and secondary

reflection of the radiated field. The use of anechoic chambers is the go-to process for such measurements. However, for novel and conceptual plasma antennas where control of low pressure gas is a monumental task, numerical modeling techniques with multi-physical coupling capability can successfully predict the antenna behaviour without sacrificing considerable accuracy. The difficulty with these models often lies within the definition of boundary conditions and selecting a suitable mesh. Care must be taken while simulating such a sensitive structure that is prone to change in impedance with even a slight variation in input power and gas pressure. Overall, this modeling scheme can be considered a powerful tool to validate any novel concept against available experimental data and further examination of electromagnetic properties of the device under consideration.

REFERENCES

- [1] Shih, Ting-Yen, and Nader Behdad. "Wideband, non-Foster impedance matching of electrically small transmitting antennas." *IEEE Transactions on Antennas and Propagation* 66.11 (2018): 5687-5697.
- [2] Abbas Semnani, Kushagra Singhal, Samsud Moon, "Impedance Matching in Small Antennas through Capacitively-Coupled Plasma Technique," 76th Annual Gaseous Electronics Conference Monday-Friday, October 9-13, 2023; Michigan League, Ann Arbor, Michigan.
- [3] www.comsol.com
- [4] Jacob, Minu M., and Daniel F. Sievenpiper. "Non-Foster matched antennas for high-power applications." *IEEE Transactions on Antennas and Propagation* 65.9 (2017): 4461-4469.
- [5] A. Semnani, K. Singhal and S. T. Moon, "A Plasma-Based Technique for Wideband Matching of Electrically Small Antennas," 2023 IEEE International Symposium on Antennas and Propagation and USNC-URSI Radio Science Meeting (USNC-URSI), Portland, OR, USA, 2023, pp. 1349-1350, doi: 10.1109/USNC-URSI52151.2023.10237701.
- [6] Moon, Samsud. "A Plasma-Based Approach for High-Power Tunable Microwave Varactors." arXiv preprint arXiv:2404.18068 (2024).
- [7] Sievenpiper, Daniel F., et al. "Experimental validation of performance limits and design guidelines for small antennas." *IEEE Transactions on Antennas and Propagation* 60.1 (2011): 8-19.
- [8] Y. P. Raizer, *Gas Discharge Physics*, Berlin: Springer-Verlag, 1991.
- [9] A. Semnani, K. Singhal and S. T. Moon, "A Plasma Matching Approach to Realize Wideband and Efficient Small Antennas," 2023 IEEE International Conference on Plasma Science (ICOPS), Santa Fe, NM, USA, 2023, pp. 1-1, doi: 10.1109/ICOPS45740.2023.10481261.